Mechanism of Action of a Membrane-Active Quinoline-Based Antimicrobial on Natural and Model Bacterial Membranes

T. M. Hubbard, Alasdair; Barker, Robert; Rehal, Reg; Vandera, Kalliopi-Kelli A.; D. Harvey, Richard; Coates, Anthony R. M.

The mechanism of action of a membrane-active quinoline-based antimicrobial on natural and model bacterial membranes

Alasdair T. M. Hubbard[1, a] · Robert Barker[3, b] · Reg Rehal[2] · Kalliopi-Kelli A. Vandera[2] · Richard D. Harvey[2, c] · Anthony R. M. Coates[1]*

[1]*Medical Microbiology, Institute for Infection and Immunity, St George's, University of London, Cranmer Terrace, London SW17 ORE, UK.*

[2]*Institute of Pharmaceutical Science, King's College London, Franklin Wilkins Building, 150 Stamford Street, London SE1 9NH, UK.*

[3]*Institut Laue Langevin, 71 avenue des Martyrs, 38042 Grenoble, France.*

Corresponding Author

*E-mail acoates@sgul.ac.uk, telephone +44 (0) 208 7255725

ABBREVIATIONS

Π, surface pressure; al-PC, 1-palmitoyl-2-[16-(acryloyloxy)hexadecanoyl]-*sn*-glycero-3-phosphorylcholine; APM, area per molecule; ATP, adenosine triphosphate; CFU, colony forming units; Chol, cholesterol; CHX, chlorhexidine; CL, cardiolipin; CW, central water; D_2O, deuterium oxide; d_{62}DPPC, 1,2-dipalmitoyl-d62-*sn*-glycero-3-phosphocholine; d_{62}DPPG, 1,2-dipalmitoyl-d62-*sn*-glycero-3-phospho-(1'-*rac*-glycerol); DiSC$_3$(5), 3,3′-dipropylthiadicarbocyanine iodide; DMSO, dimethyl sulfoxide; LB, Langmuir-Blodgett; L-PG, lysyl-phosphatidylglycerol; LS, Langmuir-Schafer; MIC, minimum inhibitory concentration; MRSA, methicillin resistant *Staphylococcus aureus*; MV, molecular volume; NR, neutron reflectometry; Pen G, penicillin G; POPC, 1-palmitoyl-2-oleoyl-*sn*-glycero-3-phosphocholine; POPG, 1-palmitoyl-2-oleoyl-sn-glycero-3-phospho-(1'-*rac*-glycerol); SAM, self-assembled monolayers; SLD, scattering length density; SMW, silicon matched water; SSI, surgical site infections; SRS, standard reaction solution; TMPA, 3-(trimethoxysilyl)propyl acrylate; TSA, tryptone soya agar.

ABSTRACT

HT61 is a quinoline-derived antimicrobial, which exhibits bactericidal potency against both multiplying and quiescent methicillin resistant and sensitive *Staphylococcus aureus,* and has been proposed as an adjunct for other antimicrobials in order to extend their usefulness in the face of increasing antimicrobial resistance. In this study we have examined HT61's effect on the permeability of *Staphylococcus aureus* membranes and whether this putative activity can be attributed to an interaction with lipid bilayers. Using membrane potential and ATP release assays, we have shown that HT61 disrupts the membrane enough to results in depolarisation of the membrane and release of intercellular constituents at concentrations above and below the minimum inhibitory concentration of the drug. Utilising both monolayer subphase injection and neutron reflectometry we have shown that increasing the anionic lipid content of the membrane leads to a more marked effect of the drug. In bilayers containing 25 mol% phosphatidylglycerol, neutron reflectometry data suggests that exposure to HT61 increases the level of solvent in the hydrophobic region of the membrane, which is indicative of gross structural damage. Increasing the proportion of PG elicits a concomitant level of membrane damage resulting in almost total destruction when 75 mol% phosphatidylglycerol is present. We therefore propose that HT61's primary action is directed towards the cytoplasmic membrane of Gram positive bacteria.

The quinoline-derived cationic antimicrobial HT61 [1] was initially developed to improve the success of nasal decolonisation interventions aimed at decreasing the risk of post-operative surgical site infections (SSI) posed by carriage of methicillin resistant *Staphylococcus aureus* (MRSA) [2, 3]. However, more recently it has been proposed as a resistance breaker to be used in conjunction with other more established antimicrobials [4]. Although the protein synthesis inhibitor mupirocin is currently widely used for anti-MRSA nasal decolonisation, it is not active against non-multiplying persister bacteria which constitute a reservoir for recolonisation [5]. In addition to this, an increased prevalence of mupirocin resistant MRSA [6] has led to the development of more effective alternatives, including the experimental antimicrobials LTX-109 [7] and XF-73 [8] in addition to HT61 [1].

The mode of action of HT61 has not hitherto been thoroughly investigated, however initial cell-based assays showed that HT61 is capable of depolarising the cytoplasmic membrane of Gram positives with further evidence from electron microscopy suggesting that HT61 causes lysis of either the membrane or cell wall [1, 4]. The putative membrane-targeting of HT61 may provide some explanation for its potency against non-multiplying MRSA [9], and suggests that its mechanism of action may be similar to those of other membrane-active antibiotics such as daptomycin [10], cationic antibiotics such as polymyxins B and E (colistin), gramicidin S [11] and cationic antimicrobials, for example chlorhexidine [12] and ceragenins [13]. In general, membrane-active cationic antimicrobials are thought to act by either binding to the headgroups of anionic membrane lipids and disrupting lipid packing to elicit increased permeability of ions and cell metabolites, or to solubilise the membrane in a detergent-like manner [12].

Initially we sought to further examine and confirm the proposed membrane disrupting capabilities of HT61 by employing two simple techniques to measure HT61's ability to damage or increase the permeability of *S. aureus* membranes, a membrane potential assay

and ATP release assay [14]. These techniques have previously been used to investigate the membrane-activity of daptomycin [15], chlorhexidine [16], ceragenins [13], telavancin [17] and oritavancin [18] in which it was determined that these antimicrobials have a direct action on bacterial membranes, resulting in membrane disruption, loss of membrane integrity and release of intracellular constituents.

In order to examine the putative membrane active mechanism of HT61 more closely, we also assessed the drug's affinity for simple staphylococcal-mimetic membrane models composed of synthetic phosphatidylcholines (PC) and phosphatidylglycerol (PG) lipids. The relative proportions of the major phospholipid species in *S. aureus* membranes are dependent upon culture conditions, but their ranges are approximately as follows; PG 30-60%, cardiolipin (CL) 5-10% and lysyl-phosphatidylglycerol (L-PG) 20-50% [19-21]. The increased biosynthesis of L-PG induced by mild environmental acidity or the presence of cationic antimicrobial peptides, is thought to attenuate the activity of membrane-active cationic antimicrobials against *S. aureus* via membrane charge dampening [22]. However, in the stationary phase, *S. aureus* membranes contain lower quantities of L-PG [23], which is likely to exist in either a zwitterionic form, or in a cationic form which would be incorporated into a neutral ion pair with PG or CL [24]. To reduce the number of variables in our model systems, the single and paired neutral lipid components of the staphylococcal membrane were represented by PC, with the excess anionic lipid content represented by PG.

An initial assessment of HT61s specificity against the simple staphylococcal membrane model was conducted by comparing the kinetics of its partitioning into lipid monolayers deposited at the air/water interface following subphase injection of the drug, before conducting the more detailed study of the effects of HT61 on lipid bilayers using solid/liquid interface neutron reflectometry (NR). The NR samples were prepared by deposition of various PC/PG mixtures onto lipid grafted silicon substrates to form floating bilayers, in

order to ensure that their thermodynamic properties more closely resembled those of biomembranes [25]. Due to the need to maintain stable planar bilayers for the NR experiments, CL was excluded form the model lipid bilayers, because of its propensity to localise in domains with negative curvature [26]. The use of chain-deuterated lipids to form the bilayers provided some contrast with the hydrogenated HT61 allowing us to determine the nature of any structural effects on the bilayers elicited by drug/membrane interaction. The complementary biological and biophysical techniques employed in this study shed light on both the bactericidal membrane-active mechanism of HT61 [4] and its specificity against staphylococci and other bacteria.

METHODS AND MATERIALS

Materials

The phospholipids 1-palmitoyl-2-oleoyl-*sn*-glycero-3-phosphocholine (POPC) (>99%), 1-palmitoyl-2-oleoyl-sn-glycero-3-phospho-(1'-*rac*-glycerol) (POPG) (>99%), 1,2-dipalmitoyl-d62-*sn*-glycero-3-phosphocholine (d_{62}DPPC) (>99%), 1,2-dipalmitoyl-d62-*sn*-glycero-3-phospho-(1'-*rac*-glycerol) (d_{62}DPPG) (>99%) and cholesterol (Chol) (>98%) were all obtained from Avanti Polar Lipids Inc. (Alabaster, AL, USA) Ultra-pure water was obtained from a Milli-Q 16 Ultra-pure water system (Merck Millipore, USA) at a specific resistivity of 18.2 MΩ.cm. HEPES, glucose, 3,3′-dipropylthiadicarbocyanine iodide (DiSC$_3$(5)), phosphate buffered saline (PBS), dimethyl sulfoxide (DMSO) and 99.9% isotopically pure deuterium oxide (D_2O) were all obtained from Sigma Aldrich (Poole, Dorset, UK). Nutrient broth, iso-sensitest broth and tryptone soya agar (TSA) all obtained from Oxoid (Basingstoke, Hampshire, UK).

The antimicrobials were used as supplied, without any additional purification and were diluted in ultrapure water. The antimicrobials used, and their stock concentrations, were as follows; chlorhexidine diacetate (10 mg/ml), penicillin G (2 mg/ml) all Sigma Aldrich (Poole, Dorset, UK), daptomycin (10 mg/ml) (Cubicin, USA) and HT61 mesylate (10 mg/ml) (Helperby Therapeutics, UK). The use of daptomycin required supplementation with 50 mg/L calcium chloride.

Bacterial Strain and Growth Conditions

Oxford *S. aureus* (NCTC 6571) was grown at 37˚C in nutrient broth at 100 rpm for either 18 hours (logarithmic growth phase) or 5 days (stationary growth phase).

Determining Antimicrobial Minimum Inhibitory Concentrations

Bacterial cultures were diluted to 0.05 OD_{600} (1×10^6 CFU/ml) in iso-sensitest broth, prior to triplicate 290 µl samples of the culture receiving 10 µl aliquots of the antimicrobials chlorhexidine, daptomycin, HT61 or penicillin G to make seven final concentrations ranging from 16-0.25 mg/L, 8-0.125 mg/L, 32-0.5 mg/L and 2-0.03 mg/L, respectively, in a 96-well microtitre plate. A blank sample of 300 µl iso-sensitest broth was added to one column and 300 µl of the untreated culture was added to the last row of the 96-well microplate (VWR, UK) to serve as a negative and positive control and incubated for 18 hours at 37˚C. The minimum inhibitory concentration (MIC) for each antimicrobial was determined as the lowest concentration at which there was no visible bacterial growth.

Membrane Potential Assay

Bacterial cultures were grown to either exponential or stationary phase as described above, prior to dilution to 0.05 OD_{600} (1×10^6 CFU/ml). The potentiometric fluorescent probe $DiSC_3(5)$ was added to each culture at a final concentration of 0.8 µM, and was given sufficient time to accumulate in the plasma membranes of the cells. Using an opaque, black 96-well microplate (Thermo Scientific, UK), 290 µl of the cell suspension with dye was added to the wells and the fluorescence intensity was measured using a Fusion 153601 fluorescence microplate reader (Perkin Elmer, UK) at excitation and emission wavelengths of 620 and 670 nm respectively, at 500 V and a gain setting of 1. In triplicate, 10 µl of the membrane-active biocide chlorhexidine, HT61 and the cell wall synthesis inhibitor penicillin G were added to the 290 µl cell suspension, making final concentrations of 32, 16, 8, 4, 2, 1 and 0.5 mg/L. To the final well, 10 µl of HEPES buffer was added as a drug-free control. The fluorescence intensity of each well was measured after a 20 minute incubation with the antimicrobials. Fluorescence intensities from the blank measurements were subtracted from the final results and the control intensities were subtracted from each time point.[4]

ATP Release Assay

After incubation to either exponential or stationary phase, bacterial cultures were centrifuged at 3600 rpm for 20 minutes and washed three times in PBS, prior to re-suspension in HEPES buffer (5 mM HEPES, 5 mM glucose, pH 7.2) and dilution to 0.2 OD_{600} ($1x10^8$ CFU/ml). Chlorhexidine, HT61 and penicillin G were added to 0.5 ml of the bacterial suspensions in centrifuge tubes to give final drug concentrations of 16, 8, 4 or 2 mg/L with ultrapure water used as the negative control. The treated cultures were incubated for 20 minutes at room temperature, and then centrifuged at 13000 rpm for 5 minutes. Following centrifugation, 200 µl of the supernatant was mixed with 200 µl of DMSO (to produce the extracellular sample) and the rest was discarded. The remaining pellet was re-suspended in 500 µl DMSO and incubated for 10 minutes at room temperature (to produce the intracellular sample), with 500 µl HEPES buffer added after incubation. Using a black 96-well microplate, 10 µl of the intracellular sample and 10 µl of the extracellular sample were added to two separate wells containing 290 µl of the luciferase-containing standard reaction solution (SRS) made according to the ATP Determination Kit instructions (Invitrogen, UK). To a separate well, 10 µl of 50% DMSO and 50% HEPES buffer was added to 290 µl of SRS. ATP-catalysed luciferase luminescence was then measured on a GloMax Multi+ microplate reader (Promega, UK). The blank sample luminescence was subtracted from all samples to mitigate the influence of natural release of ATP from the cell and the bioluminescence in 500 µl was calculated.

Lipid Monolayer Drug Partitioning

The effect of the subphase injection of HT61 on the surface pressure of biomimetic lipid monolayers was investigated using a custom-made polytetrafluoroethylene (PTFE) 110 cm^3 trough in combination with a Nima PS4 surface pressure microbalance (Nima Technologies Ltd., Coventry, U.K.) at 22°C. Three different monolayers were employed; a neutral lipid

control consisting only of POPC, a mammalian membrane mimetic control containing a POPC/Chol 75:25 molar ratio mixture and a Staphylococcal mimetic POPC/POPG 75:25 molar ratio mixture. In each case, the lipids were deposited at the air/water interface from solution in chloroform (2 mg/ml total lipid) until a surface pressure of between 30 – 35 mN/m was obtained. The surface pressure was continually monitored whilst the monolayer was allowed to achieve a stable surface pressure, before the injection into the subphase of 100 µl of HT61, from a syringe fixed prior to monolayer deposition, to give a final concentration of 9.1 µg/ml. Surface pressure changes were continually recorded until a stable plateau was achieved.

Nonlinear regression was applied to estimate the lag and slope of the Pressure-Time isotherm curves [27] generated after subphase injection of HT61. A general observation of the data is that the change in surface pressure ($\Delta\Pi$) follows a sigmoid increase over time. Both a three-parameter Hill equation and a four-parameters sigmoidal function were used to fit the data depending on which gave a better fit according to the correlation coefficient obtained. The three-parameter Hill equation is described by the formula:

$$\Delta\Pi = \frac{\Delta\Pi_{max} \cdot t^H}{t_{50}^H + t^H} \qquad\qquad (1)$$

Where t represents the time, $\Delta\Pi_{max}$ denotes the maximum change in surface pressure, H is the Hill coefficient and t_{50} is the time taken to achieve 50% of the $\Delta\Pi_{max}$.

The four-parameters sigmoidal model is described by the following function:

$$\Delta\Pi = \Delta\Pi_0 + \frac{\Delta\Pi_{max} - \Delta\Pi_0}{e^{-(t - t_{50}/H)}} \qquad\qquad (2)$$

Where $\Delta\Pi_0$ denotes the minimum $\Delta\Pi$ (lower plateau/asymptote).

In both models the Hill coefficient describes the overall growth rate of the curve and is a measure of how quickly the curve moves from the lower asymptote to the upper asymptote.

Neutron Reflectivity at the Solid/Liquid Interface

The interaction of HT61 with the lipids of bacterial membrane mimetic bilayers was further investigated by solid/liquid interface neutron reflectometry using the D17 beamline at the Institut Laue-Langevin (Grenoble, France) [28]. The samples were deposited as bilayers onto silicon substrates measuring $50 \times 80 \times 10$ mm (Crystran Ltd, Poole, UK), the single polished surface (5 Å RMS roughness tolerance) which had previously been functionalised with covalently bound 3-(trimethoxysilyl)propyl acrylate (TMPA) and 1-palmitoyl-2-[16-(acryloyloxy)hexadecanoyl]-*sn*-glycero-3-phosphorylcholine (al-PC), based on the method of Hughes *et al.* [29]. This functionalised surface is henceforth referred to as the al-PC self-assembled monolayer (al-PC SAM). Prior to bilayer deposition, the al-PC SAM layers where fully characterised on the D17 reflectometer at two different angles (0.8° and 3.2°) in H_2O, silicon matched water (SMW) (62% v/v H_2O and 38% D_2O) and D_2O contrasts.

Bilayers consisting of d_{62}DPPC and d_{62}DPPG mixtures in molar ratios of 75:25, 50:50, and 25:75 were deposited onto the al-PC SAMs by means of sequential Langmuir-Blodgett (LB) and Langmuir-Schafer (LS) techniques (ratio of 1:1), using a Nima 1212D Langmuir trough (Nima Technologies, UK) with an automated dipping mechanism [25]. The appropriate d_{62}DPPC/d_{62}DPPG mixtures were deposited onto an ultrapure water subphase from a 1 mg/ml solution in chloroform, the solvent was allowed to evaporate and then the monolayer compressed to achieve a surface pressure of 28 mN/m at 25°C. A previously submerged SAM-coated silicon block was removed from the dipping well using the automated arm at a rate of 5 mm/minute, to deposit the inner leaflet of the d_{62}DPPC/d_{62}DPPG bilayer. To deposit the outer leaflet lipids, the silicon block was turned through 90°, so that the SAM and deposited inner leaflet were parallel with the water surface, and lowered back into the dipping well at a rate of 3 mm/minute.

The floating bilayers were sealed, while still submerged, into their solid-liquid sample cells, to ensure that the SAM and bilayer were not exposed to air. The sample cell had two valves on opposite sides and a small reservoir inside (which was filled with water) to allow for solvent exchange during the reflectivity experiment.

The cells containing the various SAM and bilayer combinations were mounted onto automated sample changer on the D17 reflectometer. The samples were characterised at 55°C (to ensure acyl chain fluidity and thus give results comparable with those obtained for the monolayer partitioning studies) at two different angles of 0.8° and 3.2°. Neutron reflectometry data was collected again against three solvent contrasts; H_2O, SMW and D_2O. The solvents were exchanged automatically using a Knauer Smartline HPLC pump 1050 (Berlin, Germany). After the characterisation of the bilayers, HT61 was added to the samples in two aliquots. Initially 10 ml of 1.67 µg/ml HT61 in H_2O was pumped into each of cells and the data was collected in the same way as the sample characterisation outlined above. A further 20 ml of 1.67 µg/ml HT61, was pumped into each cell before further data collection.

The data obtained from the neutron reflectivity measurements was analysed using custom procedures with the RasCAL software package [30]. The grafted al-PC SAM was characterised in the absence of the floating bilayers, by fitting them as a four layer model consisting of the following components extending from the silicon substrate; a layer of silicon oxide (SiO_2), the TMPA linker layer, the al-PC hydrocarbon chains (al-PC Chains) and the al-PC headgroups (al-PC Heads). The scattering length density (SLD) values for each of these layers was fixed using values obtained from Hughes *et al.* [29]. The proportion of the silicon substrate which was covered by the SAM was determined by quantifying the solvent penetration into the al-PC chains region (Table S1). Solvent present in the al-PC layer would be expected to be displaced by lipid during the subsequent deposition of the floating bilayer. Thus an 'al-PC filling in' parameter is used when fitting the data obtained from the deposited

floating bilayers. After deposition of the floating bilayer, the coverage of the SAM is therefore effectively 100% due to this filling of any inhomogeneity with the deposited lipids.

The reflectivity curves obtained from the samples with floating bilayers were fitted simultaneously from the measurements recorded in each of the three different solvent contrasts (with the parameters for the al-PC SAM constrained by the fitted data for the substrate alone). The parameters used to fit the floating bilayer were the separation distance between the al-PC SAM and the deposited bilayer (Central Water or CW thickness), the area per molecule (APM) of the lipids in the deposited bilayer, the number of water molecules associated with the headgroups (H_2O_{head}) and the tails (H_2O_{tail}) of each lipid molecule and the roughness of the system (both local and global). This approach to fitting the data is more constrained by the physical parameters of the lipid membrane and requires fewer parameters to fit than a standard layer approach used elsewhere [31]. Parameterisation of building on the membrane has previously been discussed by Tatur *et al.* [32], here the number of water molecules per head and tail was calculated assuming that any change in the SLD of the layer towards the SLD of the solvent was due to penetration of the solvent into the layer. Using the number of water molecules (NW) per head and tail and the molecular volume of the lipids, the SLD of each layer in the bilayer was calculated using:

$$\mathrm{SLD}_{layer} = \frac{\sum b_{lipid} + (\mathrm{NW}_{layer} \cdot b_{solvent})}{\sum \mathrm{MV}_{lipid} + (\mathrm{NW}_{layer} \cdot \mathrm{MV}_{solvent})} \qquad (3)$$

Further, the thickness of each layer was calculated from the APM and number of water molecules in the layer using:

$$L_{layer} = \frac{\sum \mathrm{MV}_{lipid} + (\mathrm{NW}_{layer} \cdot \mathrm{MV}_{solvent})}{\mathrm{APM}} \qquad (4)$$

where the molecular volumes (MV) and scattering cross sections (b) of each of the individual components in the system were calculated from literature values [33, 34].

The additional tail hydration parameter, stated in Table 3, is a direct representation of the coverage of the floating bilayer and was calculated from the fitted parameters using the equation:

$$\text{Tail Hydration} = \frac{\text{MV}_{solvent} \cdot \text{H}_2\text{O}_{tail}}{\text{MV}_{tail} + (\text{MV}_{solvent} \cdot \text{H}_2\text{O}_{tail})} \times 100 \qquad (5)$$

where the percentage coverage of the floating bilayer is given by subtracting the Tail Hydration from 100. The errors stated are the result of Monte Carlo error analysis within RasCAL, known as 'bootstrapping' errors [35]. This approach to estimating errors involves finding the distribution of values for each parameter fitted as a function of the initial starting values. For all the errors presented the minimisation was repeated 200 times with randomised starting values fitted to a randomised number of points within the raw data, the standard deviation error of possible values for each parameter based on this was then found.

RESULTS

Minimum Inhibitory Concentrations

The MICs for the antimicrobials used in this study were as follows; HT61 8 mg/L, chlorhexidine 4 mg/L, daptomycin 2 mg/L and penicillin G 0.5 mg/L. All the antimicrobials used during this study were therefore confirmed to have activity against *S. aureus*. The MIC of HT61 was higher in comparison to the other antimicrobials used, which was in agreement with the previously published MIC of HT61 against the same *S. aureus* strain.[1]

Membrane Potential Assay

Membrane depolarisation caused by structural perturbations, can be measured using the amphiphilic and cationic potentiometric fluorescent probe DiSC$_3$(5). When partitioned into a cell membrane, DiSC$_3$(5) fluorescence is quenched in the presence of a resting potential and

once released back into free solution following membrane damage, the fluorescence is dequenched [36, 37].

Both chlorhexidine and HT61 disrupted the *S. aureus* membranes to a large enough degree to cause depolarisation in both logarithmic (Fig. 1a) and stationary phase (Fig. 1b) cells in a concentration-dependent manner, a result which is consistent with previous findings [1, 16]. At the highest concentration used, penicillin G did not depolarise the *S. aureus* membranes (Fig. 1) which is consistent with its mode of action requiring longer than 20 minutes to achieve cell lysis [14]. As the concentration of HT61 and chlorhexidine increases above the MIC, HT61 caused a higher degree of depolarisation, and therefore we might surmise disrupted the membrane to a greater degree than chlorhexidine.

To compare the rates of depolarisation (*Vdep*) of the different antimicrobials, the initial rate of depolarisation over the first minute after challenge was calculated and plotted against antimicrobial concentration, using a sigmoidal Hill function (eqn 6) fitted to the experimental data (using the non-linear curve fitting function in OriginLab Corp. Origin Pro 2016 Sr1):

$$Vdep = Vdep_{min} + \frac{Vdep_{max} - Vdep_{min} \cdot D^H}{K_m^H + D^H} \qquad (6)$$

As a means of comparing the activities of each drug, the maximum rate of depolarisation (*V*dep$_{max}$) was determined in addition to the Michaelis-Menten constant (*K$_m$*) which denotes the drug concentration (*D*) needed to achieve half of the maximum rate of depolarisation. The Hill coefficient (*H*) gives an indication of the overall rate of change across the full drug concentration range. The initial rate of depolarisation over the first minute for logarithmic and stationary phase *S. aureus* caused by chlorhexidine and HT61 was entirely concentration dependent (Fig. 2). Membrane disruption by HT61 depolarised the membranes of both the logarithmic (*Vdep$_{max}$* 21.0 s^{-1}, *K$_m$* 5.8 μg/ml) and stationary phase (*Vdep$_{max}$* 10.9 s^{-1}, *K$_m$* 3.5 μg/ml) *S. aureus* cells faster and to a greater degree than chlorhexidine did in each case,

especially below the MIC (logarithmic phase; $Vdep_{max}$ 6.3 s^{-1}, K_m 11.8 μg/ml and stationary phase; $Vdep_{max}$ 10.1 s^{-1}, K_m 4.8 μg/ml). It is interesting to note that the activity of HT61 is attenuated to a greater degree in the stationary phase cells, compared to that of chlorhexidine.

ATP Release Assay

Substantial damage to cell membranes generally causes a rapid loss of large cellular components, such as ATP [14, 38]. As expected, penicillin G caused little to no release of ATP from the cells after 20 minutes (Fig. 3a and 3b), as this is not sufficient time for it to cause lysis through cell wall synthesis inhibition [14].

The membrane disruption caused by chlorhexidine and HT61, as indicated in the depolarisation assay, was indeed sufficient to induce the release of between approximately 11% (at a concentration of 8 μg/ml chlorhexidine) and 71% ATP (at a concentration of 16 μg/ml HT61) from logarithmic phase cells, but there was no release of ATP at lower concentrations (Fig. 3a). There was a larger degree of membrane disruption by HT61 and chlorhexidine towards stationary phase cells compared to logarithmic phase cells, resulting in a larger release of between approximately 36% and 88% ATP (Fig. 3b).

Lipid Monolayer Drug Partitioning

Having established that HT61 exhibits a lytic action on the *S. aureus* plasma membrane, from the results of biochemical whole cell based assays, the subsequent biophysical experiments using synthetic membrane mimetic models concentrated solely on examining this putative mode of action of HT61 in greater detail. There are marked differences in the kinetics of the interaction of subphase-injected HT61 and monolayers with different lipid compositions deposited at the air/water interface (Figure 4). The lack of any appreciable change in surface pressure when the net neutral charged POPC monolayer was exposed to HT61, indicates that charge plays an important role in initiating the interaction of the drug with lipid membranes.

The addition of 25 mol% cholesterol to the POPC monolayer does elicit some interaction with HT61, which is sufficient to allow modelling of the kinetics with the three-parameter Hill function (equation 1). However, in the presence of sterol the maximum change in surface pressure for the POPC/Chol monolayers remained modest at 2.9 mN/m (Table 1) and the Hill coefficient of 1.04 indicates that the overall rate of surface pressure change is comparatively low. It is possible that some roughness of the monolayer caused by the inclusion of the sterol allows for some hydrophobic interaction with the HT61, which for the most part is sterically excluded from the interface by the presence of the cholesterol intercalated between the lipid molecules. Due to the minimal interaction HT61 had with the POPC and POPC/Chol monolayers, these lipid compositions were omitted from the subsequent neutron reflectivity experiments.

The interaction of HT61 with the POPC/POPG monolayer is markedly different from its behaviour in the presence of the neutral monolayers. The inclusion of the anionic POPG in the monolayer resulted in a large increase in surface pressure following injection of the drug (Figure 4). The surface pressure changes elicited by the interaction show a biphasic pattern, the two phases of which were modelled in an overlapping piecewise fashion using both the three-parameter Hill function, between 0 and 35 s, and the four-parameter sigmoidal function (equation 2) between 17 and 300 s (Table 1). The biphasic nature of the interaction may result from the slow diffusion of the HT61 in the large bulk volume limiting the rate of partitioning during the first ~50 s post injection. Nevertheless when compared with the POPC/Chol monolayer, the HT61 interacts much faster with the POPC/POPG mixture and much more rapidly during the first phase (Hill coefficient 1.40). The maximum change in surface pressure of 13.7 mN/m, at the end of the second phase indicates that the monolayer allows the drug to partition and access the air/water interface at a very rapid rate (Hill coefficient 8.77). The main assumptions which can be drawn from these results are that it is

the presence of the charged POPG that drives the initial attraction between the monolayer and the drug and encourages the partitioning of the drug via hydrophobic interactions.

Neutron Reflectivity

The fitted structural characteristics of each of the al-PC SAM layers used in this study are available to view in the supporting information. The grafted lipid coverage of each of the blocks was ~70%, as determined from the al-PC chains percentage hydration. The backfilling of regions not covered by the al-PC, which would have occurred by transfer from the lipid monolayer during the LB deposition step, was incorporated into the fitting for each of the floating bilayers, together with the fixed SAM parameters (Supporting Information). The values for the parameters used in the fitting of three floating d_{62}DPPC/d_{62}DPPG bilayers (Fig. 5), together with those calculated using them (equations 3, 4 and 5), are compiled in Table 2. Characterisation of the floating bilayer before and after challenge with HT61 was performed at 55°C to ensure that the bilayer lipids would be in the fluid phase, making the data obtained from the model comparable with those obtained from the POPC/POPG mixtures used in the monolayer study. It should be noted that the method used to fit the parameters of the floating bilayer, whereby reflectivity data obtained from three solvent contrasts (H_2O, SWM and D_2O) were fitted simultaneously (see Supporting Information Figs S2, S3 and S4), some deviation from the experimentally obtained curves is inevitable (Fig. 5). Although this serves to highlight that the parameters incorporated into the fitting routine may not have been entirely comprehensive, the error incurred nevertheless ensured that the fitted parameters were maintained within a physically reasonable range.

There are three noteworthy effects of increasing the % d_{62}DPPG in these bilayers. The separation between the SAM and the floating bilayer (CW thickness), was found to increase dramatically at and above 50 mol % d_{62}DPPG. The reason for this increase is not clear, however it is of a magnitude similar to those found between bilayers of like charge [39]. The

second noteworthy difference between the floating bilayers is in their calculated thicknesses, which decrease from ~44 Å in the 25 mol % d_{62}DPPG to ~36 Å when the amount of d_{62}DPPG was increased to 50 mol%. In the case of the 75 mol % d_{62}DPPG the fitting suggests that there is significant thinning of the bilayer to ~28 Å which appears to be of a magnitude consistent with lipid chain interdigitation [40]. There is however, little difference in the calculated tail hydration, which can be used as a measure of floating bilayer integrity, since it suggests close to complete coverage for each of the lipid mixtures. Finally, the closest packed (based on APM) and lowest degree of undulation membrane (indicated by the global roughness) was found for the [50:50] d_{62}DPPC/d_{62}DPPG mixture. It might be suggested that this ratio of charged to zwitterionic species in the membrane offers the best packing of the lipids in this bilayer and thus the membrane fluctuations are reduced. However, this experimental data cannot shed any further light on to this phenomenon.

The first clear effect of the interaction with the lipids of the bilayer following HT61 challenge is a consistent reduction in the separation distance between the floating bilayer and the SAM (central water thickness), which is independent of PG content in the membrane (Fig. 5D, E, F and Table 2). This could be due to the addition of HT61 resulting in a change in the overall charge of the bilayer by partitioning into the membrane and neutralising the anionic charge of d_{62}DPPG present in both leaflets and therefore eliciting a decrease in the central water thickness due to reduced repulsions. Additionally, there is no decrease in the bilayer fluctuations, suggesting that the change in central water thickness after addition of HT61 is more likely due to a reduced electrostatic contribution, and not a reduction in Helfrich type steric repulsion between the two surfaces [41].

The addition of the first injection of HT61 to bilayers containing only 25% d_{62} DPPG resulted in a thinning of the bilayer by ~6 Å a phenomenon which has previously been observed using NR for bilayers composed of similar PC/PG ratios upon challenge with the antimicrobial

peptide aurein [42]. Overall the most significant effect of HT61 challenge on the lipids in the bilayer is evident in the increase in both APM and percentage tail hydration, indicating that material was lost from the bilayer and replaced by the solvent (Table 2). Since the two doses of HT61 led to similar effects, with an increase in magnitude with each addition of the drug, this provides the best evidence for a structural change in the bilayer directly induced by the drug. Increasing the proportion of d_{62}DPPG in the bilayer apparently resulted in further structural disruption following exposure to HT61. With respect to the derived parameters, the trend of increasing percentage tail hydration would again suggest that the coverage of the floating bilayer is decreasing and thus that exposure to the drug results in loss of material through structural damage to the system. At 75% anionic lipid content the magnitude of the HT61 structural effects upon the floating bilayer was at its greatest. Here, the second addition of HT61 seems to result in an almost total loss of the floating bilayer, with an apparent final coverage of only 30%. It should be noted that the difference between the raw data and the model fits in the H_2O, SMW and D_2O contrasts following challenge with HT61 and the higher error in the membrane hydration after addition of the drug results from the significant disruption of the bilayer, the model used to fit these data finds it difficult to constrain when the bilayer is almost completely removed. However, the structural trend is nevertheless quite clear; the introduction of HT61 to the bilayers leads to the removal of lipids from the membrane and significant disruption at magnitudes which directly correlate with the amount of PG in the membrane.

DISCUSSION

Direct action on bacterial membranes has been implicated as the primary mode of action for a number of different antimicrobials, including chlorhexidine,[16] daptomycin[15] and telavancin.[17] Previous investigations into these membrane-active antimicrobials have typically used antimicrobial concentrations 1 to 8 times the MIC [15, 17, 43, 44], however in this

study we have used concentrations above and below the MIC of HT61 towards *S. aureus* to investigate the true level of membrane-activity of HT61 compared to other membrane-active antimicrobials. All assays used for measuring membrane damaging effects were run over a short time frame [14] as membrane damage over a longer time frame may be due to a side effect of an alternative mode of action.

Previous studies of daptomycin [15, 43], ceragenins[13] and telavancin[17] have shown that they are able to depolarise Gram positive bacterial membranes and elicit the release of intracellular components, such as K^+ and ATP, in a concentration-dependent manner. As previously shown by Castillo *et al.* [16] chlorhexidine increased the permeability of logarithmic phase *S. aureus* membranes, leading to depolarisation and release of ATP. In this study, we found that not only did depolarisation and ATP release occur in a concentration dependent manner in logarithmic *S. aureus*, but that this also occurs in stationary phase cells, and we were able to determine the initial rate at which depolarisation occurred. HT61's ability to disrupt and increase the permeability of the membrane, similar to other membrane-active antimicrobials, was confirmed by the rapid, concentration dependent depolarisation of *S. aureus* membranes and the significant release of ATP, to a greater degree than chlorhexidine. HT61's superior interaction with non-multiplying bacteria, proposed by Hu *et al.* [1] was also confirmed due to a faster rates of depolarisation and larger ATP release at the same concentrations. It is tempting to speculate that this is due to a lack of upregulated membrane defences in the stationary phase cells.

The results of this study suggest that the activity of both chlorhexidine and HT61 was superior when the cells were in stationary phase. The *S. aureus* membrane is mainly comprised of three phospholipids, the anionic lipids PG and CL, and the cationic lipid L-PG [45, 46]. It has been previously suggested that chlorhexidine non-specifically targets anionic lipids in the membrane [47] as the higher abundance of the anionic lipid PG in stationary phase

S. aureus results in an increase in activity of chlorhexidine on the membrane. L-PG is synthesised by the addition of lysine onto a PG lipid by the enzyme MprF [48, 49], encoded by the *mprF* gene. *mprF* is strongly expressed in logarithmic phase *S. aureus* but downregulated in stationary phase *S. aureus* [23] due to a change in metabolic activity when *S. aureus* moves from the exponential phase to the stationary phase. This results in a higher abundance of anionic lipids in the stationary phase membranes. From the evidence of this study, the effect of HT61 on the membranes of *S. aureus* in two different growth phases seems to be similar to that of chlorhexidine, therefore, it is proposed that HT61 also non-specifically targets the anionic lipid in a membrane.

The extent to which HT61 alters and ultimately disrupts lipid membrane structure appears to be directly proportional to their anionic lipid content, suggesting that Coulombic forces are the main drivers of the drug-membrane interaction. The evident ability of HT61 to cause major damage to the membrane by destroying membrane integrity, indicates that the hydrophobic properties of the drug also constitute an essential factor for its membrane-activity. The results reported in this study offer some insight into the various stages involved in structural changes induced by HT61 upon challenge to susceptible lipid bilayers.

From the results of the Langmuir monolayer experiments, it is evident that HT61 is not only attracted to monolayers containing anionic lipids, but it also readily partitions into these monolayers. The lack of interaction observed with the POPC monolayers reliably demonstrates that net neutral lipids elicit no such attraction. It is interesting to note that a similar partitioning study examining the interaction between chlorhexidine and DPPC monolayers observed an increase of ~5 mN/m [47], suggesting that the biocide has some interaction with the interfacial region PC membranes, an observation corroborated by neutron diffraction studies on PC bilayers [50]. The minimal and gradual increase in surface pressure observed in the case of the mammalian membrane mimetic POPC/Chol monolayer may have

arisen due to monolayer packing inconsistencies caused by the inclusion of the sterol, which would be likely to allow some degree of hydrophobic interaction with the drug. Since this is negligible compared to the rapid and strong interaction observed in the POPC/POPG which were of comparable magnitude to surface pressure changes observed for chlorhexidine and daptomycin interactions with similar lipid monolayers [47, 51], the presence of anionic lipid is clearly the major determinant for HT61 binding and partitioning and provided the rationale for not continuing with the POPC and POPC/Chol systems in subsequent experiments. The structural consequences of HT61 partitioning into PG-containing membranes was observed in more detail from our neutron reflectivity studies.

The NR data shows that prior to exposure to HT61, the separation between SAM and floating bilayer (CW thickness) of the three bilayers increased as the content of d_{62}DPPG increased. The CW thickness or separation, is maintained by a balance of attractive and repulsive forces between the floating bilayer and the al-PC SAM [29]. Van der Waals forces created by interaction of the al-PC with the zwitterionic d_{62}DPPC of the bilayer, will create the attractive forces bringing the bilayer closer to the SAM. However, the repulsive forces have been suggested to be created by one of two ways, either by a hydration force or fluctuation pressure [29]. Hydration forces can be created by the protrusion of the lipid headgroups out of the bilayer perturbing the water structure at the lipid-water interface or the partial charge transfer between polar headgroups with the water molecules [52]. The repulsion caused by fluctuation pressure are entropic factors facilitated by membrane undulations (Global Roughness), single molecule protrusions and headgroup steric overlap [53-55]. Although the overall surface charge of the al-PC SAM can be considered to be neutral due to the zwitterionic al-PC monolayer, the different overall negative charges of the three bilayers still seem to have been capable of eliciting some charged repulsion between the two layers [56]. The addition of HT61 to these membranes showed a consistent reduction in this spacing, it is

likely that this is due to the removal of charged material from the bilayer, resulting in significant disruption of the membrane, increasing the area per molecule and reducing the repulsive contribution from the surface.

As expected, the packing and organisation of the lipids within each bilayer varied between the three different ratios of d_{62}DPPC and d_{62}DPPG, most notable was the inferred thinning of the bilayer as the amount of d_{62}DPPG present in the bilayer increased. This suggests that as the content of d_{62}DPPG increased there was some degree of interdigitation of the two leaflets due to the charged lateral repulsion between anionic head groups of d_{62}DPPG, [57, 58] which seems likely as a DPPC-only fluid bilayer has a thickness of 38 Å, [59] whereas both the 50:50 and 25:75 bilayers were thinner. The apparent interdigitation between the two leaflets may have resulted in a decrease in the APM, but the high d_{62}DPPG content in the 25:75 bilayer leads to some charged lateral repulsion, slightly increasing the APM in comparison to the 50:50 bilayer [57].

As the bilayers were very tightly packed, resulting in a low APM and percentage solvent in each prior to challenge with the drug, it is possible to infer that some gross membrane damage occurs as a result of interaction with HT61. As the d_{62}DPPG content and concentration of HT61 increased, the bilayer was more severely affected, resulting in a significant reduction in floating membrane coverage. This can be interpreted as a loss of bilayer lipid due to the membrane damaging effect of the drug. Following the second addition of HT61 to the 25:75 d_{62}DPPC/d_{62}DPPG bilayer the damage appears much more extensive, with complete destruction of the bilayers containing more charged material.

The neutralisation of the anionic lipids within the inner leaflet of the bilayer, resulting in a decrease in the separation distance between the SAM and the floating bilayer, suggests that not only does HT61 partitions into and disrupt the membrane but may also translocate across the bilayer. Whether or not such a proposed translocation can occur in lipid bilayers of a

more complex biomimetic composition than our simplified binary mixture model (i.e. including LPG and CL), will need to be examined in order to obtain more compelling evidence of the overall mechanism of the drug's action against bacterial cells. However it could be that HT61's membrane activity is only an initial mode of action and that it may have a second target within the cell itself, although this would not explain the rapid bactericidal activity of the drug [1] and this currently remains a speculative assumption which warrants further investigation.

CONCLUSIONS

Cationic HT61 is attracted to negatively charged bilayers, partitioning into them (potentially translocating across the membrane) and causing structural changes which result in the loss of membrane integrity leading to depolarisation, and ultimately severe membrane damage which elicits the release of ATP. The action of HT61 on the bilayer is dependent on its concentration and the amount of anionic lipid present, as increasing the phosphatidylglycerol content elicits a more significant loss of material and catastrophic damage to PC/PG mixed bilayers.

SUPPORTING INFORMATION

Figure S1 Initial rate of depolarisation over the first minute of both HT61 (filled triangles) and chlorhexidine (filled squares) plotted against drug concentration for logarithmic phase daptomycin resistant *S. aureus*. Error bars represent the standard error of the mean (n=3). The curves are fitted with the sigmoidal Hill function described in eqn 6. The kinetic parameters obtained from the curve fitting were in the case of HT61; $Vdep_{max}$ 11.8 s^{-1}, K_m 5.2 µg/ml and for chlorhexidine; $Vdep_{max}$ 4.7 s^{-1}, K_m 25.9 µg/ml.

Table S1 Parameters of the characterisation of the three SAM layers (indicating the specific floating bilayer with which they were associated) obtained from their fitted reflectivity profiles.

Figure S2 Fitted neutron reflectivity curves and derived SLD profiles for the SAM and floating d_{62}DPPC/d_{62}DPPG [75:25] bilayer pre and post addition of HT61.

Figure S3 Fitted neutron reflectivity curves and derived SLD profiles for the SAM and floating d_{62}DPPC:d_{62}DPPG [50:50] bilayer pre and post addition of HT61.

Figure S4 Fitted neutron reflectivity curves and derived SLD profiles for the SAM and floating d_{62}DPPC:d_{62}DPPG [25:75] bilayer pre and post addition of HT61.

AUTHOR INFORMATION

Present Addresses

[a]*Nuffield Department of Clinical Medicine, University of Oxford, Oxford, United Kingdom OX3 9DU*

[b]*School of Science and Engineering, University of Dundee, Dundee DD1 4HN, UK.*

[c]*Institute of Pharmacy, Martin Luther University Halle-Wittenberg, Halle (Saale), Germany.*

Author Contributions

The manuscript was written through contributions of all authors. All authors have given approval to the final version of the manuscript.

REFERENCES

1. Hu, Y., Shamaei-Tousi, A., Liu, Y., and Coates, A. (2010) A new approach for the discovery of antibiotics by targeting non-multiplying bacteria: a novel topical antibiotic for staphylococcal infections, *PLoS One, 5, (7),* e11818.

2. Munoz, P., Hortal, J., Giannella, M., Barrio, J.M., Rodriguez-Creixems, M., Perez, M.J., Rincon, C., and Bouza, E. (2008) Nasal carriage of *S. aureus* increases the risk of surgical site infection after major heart surgery, *J. Hosp. Infect., 68, (1),* 25-31.

3. Tai, Y.J., Borchard, K.L.A., Gunson, T.H., Smith, H.R., and Vinciullo, C. (2013) Nasal carriage of *Staphylococcus aureus* in patients undergoing Mohs micrographic surgery is an important risk factor for postoperative surgical site infection: A prospective randomised study, *Aust. J. Dermatol., 54, (2),* 109-114.

4. Hu, Y. and Coates, A.R. (2013) Enhancement by novel anti-methicillin-resistant *Staphylococcus aureus* compound HT61 of the activity of neomycin, gentamicin, mupirocin and chlorhexidine: in vitro and in vivo studies, *J. Antimicrob. Chemother., 68, (2),* 374-384.

5. Coates, T., Bax, R., and Coates, A. (2009) Nasal decolonization of *Staphylococcus aureus* with mupirocin: strengths, weaknesses and future prospects, *J. Antimicrob. Chemother., 64, (1),* 9-15.

6. Patel, J.B., Gorwitz, R.J., and Jernigan, J.A. (2009) Mupirocin Resistance, *Clin. Infect. Dis., 49, (6),* 935-941.

7. Nilsson, A.C., Janson, H., Wold, H., Fugelli, A., Andersson, K., Hakangard, C., Olsson, P., and Olsen, W.M. (2015) LTX-109 Is a Novel Agent for Nasal Decolonization of Methicillin-Resistant and -Sensitive *Staphylococcus aureus*, *Antimicrob. Agents Chemother., 59, (1),* 145-151.

8. Farrell, D.J., Robbins, M., Rhys-Williams, W., and Love, W.G. (2010) In vitro activity of XF-73, a novel antibacterial agent, against antibiotic-sensitive and - resistant Gram-positive and Gram-negative bacterial species, *Int. J. Antimicrob. Agents, 35, (6),* 531-536.

9. Hurdle, J.G., O'Neill, A.J., Chopra, I., and Lee, R.E. (2011) Targeting bacterial membrane function: an underexploited mechanism for treating persistent infections, *Nat. Rev. Microbiol., 9, (1),* 62-75.

10. Chen, Y.F., Sun, T.L., Sun, Y., and Huang, H.W. (2014) Interaction of Daptomycin with Lipid Bilayers: A Lipid Extracting Effect, *Biochem., 53, (33),* 5384-5392.

11. Zhang, L.J., Dhillon, P., Yan, H., Farmer, S., and Hancock, R.E.W. (2000) Interactions of bacterial cationic peptide antibiotics with outer and cytoplasmic membranes of *Pseudomonas aeruginosa*, *Antimicrob. Agents Chemother., 44, (12),* 3317-3321.

12. Gilbert, P. and Moore, L.E. (2005) Cationic antiseptics: diversity of action under a common epithet, *J. Appl. Microbiol., 99, (4),* 703-715.

13. Epand, R.F., Pollard, J.E., Wright, J.O., Savage, P.B., and Epand, R.M. (2010) Depolarization, bacterial membrane composition, and the antimicrobial action of ceragenins, *Antimicrob. Agents Chemother., 54, (9),* 3708-3713.

14. O'Neill, A.J., Miller, K., Oliva, B., and Chopra, I. (2004) Comparison of assays for detection of agents causing membrane damage in *Staphylococcus aureus*, *J. Antimicrob. Chemother., 54, (6),* 1127-1129.

15. Silverman, J.A., Perlmutter, N.G., and Shapiro, H.M. (2003) Correlation of Daptomycin Bactericidal Activity and Membrane Depolarization in *Staphylococcus aureus*, *Antimicrob. Agents Chemother., 47, (8),* 2538-2544.

16. Castillo, J.A., Clapes, P., Infante, M.R., Comas, J., and Manresa, A. (2006) Comparative study of the antimicrobial activity of bis(Nalpha-caproyl-L-arginine)-1,3-propanediamine dihydrochloride and chlorhexidine dihydrochloride against *Staphylococcus aureus* and *Escherichia coli*, *J. Antimicrob. Chemother., 57, (4),* 691-698.

17. Higgins, D.L., Chang, R., Debabov, D.V., Leung, J., Wu, T., Krause, K.M., Sandvik, E., Hubbard, J.M., Kaniga, K., Schmidt, D.E., Jr., Gao, Q., Cass, R.T., Karr, D.E., Benton, B.M., and Humphrey, P.P. (2005) Telavancin, a multifunctional lipoglycopeptide, disrupts both cell wall synthesis and cell membrane integrity in methicillin-resistant *Staphylococcus aureus*, *Antimicrob. Agents Chemother., 49, (3),* 1127-1134.

18. Belley, A., Neesham-Grenon, E., McKay, G., Arhin, F.F., Harris, R., Beveridge, T., Parr, T.R., Jr., and Moeck, G. (2009) Oritavancin kills stationary-phase and biofilm *Staphylococcus aureus* cells in vitro, *Antimicrob. Agents Chemother., 53, (3),* 918-925.

19. Roy, H. (2009) Tuning the properties of the bacterial membrane with aminoacylated phosphatidylglycerol, *IUBMB Life, 61, (10),* 940-953.

20. Gould, R.M. and Lennarz, W.J. (1970) Metabolism of Phosphatidylglycerol and Lysyl Phosphatidylglycerol in *Staphylococcus aureus*, *J. Bacteriol., 104, (3),* 1135-1144.

21. Mukhopadhyay, K., Whitmire, W., Xiong, Y.Q., Molden, J., Jones, T., Peschel, A., Staubitz, P., Adler-Moore, J., McNamara, P.J., Proctor, R.A., Yeaman, M.R., and Baye, A.S. (2007) In vitro susceptibility of *Staphylococcus aureus* to thrombin-induced platelet microbicidal protein-1 (tPMP-1) is influenced by cell membrane phospholipid composition and asymmetry, *Microbiol., 153,* 1187-1197.

22. Li, M., Cha, D.J., Lai, Y., Villaruz, A.E., Sturdevant, D.E., and Otto, M. (2007) The antimicrobial peptide-sensing system aps of *Staphylococcus aureus*, *Mol. Microbiol., 66, (5),* 1136-1147.

23. Matsuo, M., Oogai, Y., Kato, F., Sugai, M., and Komatsuzawa, H. (2011) Growth-phase dependence of susceptibility to antimicrobial peptides in *Staphylococcus aureus*, *Microbiol., 157, (Pt 6),* 1786-1797.

24. Tocanne, J.F., Ververga.Ph, Verkleij, A.J., and Vandeene.Ll (1974) Monolayer and Freeze-Etching Study of Charged Phospholipids .1. Effects of Ions and Ph on Ionic Properties of Phosphatidylglycerol and Lysylphosphatidylglycerol, *Chem. Phys. Lipids, 12, (3),* 201-219.

25. Barker, R.D., McKinley, L.E., and Titmuss, S. (2016) Neutron Reflectivity as a Tool for Physics-Based Studies of Model Bacterial Membranes, *Adv. Exp. Med. Biol., 915,* 261-282.

26. Strandberg, E., Zerweck, J., Wadhwani, P., and Ulrich, A.S. (2013) Synergistic insertion of antimicrobial magainin-family peptides in membranes depends on the lipid spontaneous curvature, *Biophys. J., 104, (6),* L9-11.

27. Bello, G., Bodin, A., Lawrence, M.J., Barlow, D., Mason, A.J., Barker, R.D., and Harvey, R.D. (2016) The influence of rough lipopolysaccharide structure on molecular interactions with mammalian antimicrobial peptides, *Biochim. Biophys. Acta, 1858, (2),* 197-209.

28. Cubitt, R. and Fragneto, G. (2002) D17: the new reflectometer at the ILL, *Appl. Phys. A: Mater. Sci. Process., 74,* S329-S331.

29. Hughes, A.V., Howse, J.R., Dabkowska, A., Jones, R.A.L., Lawrence, M.J., and Roser, S.J. (2008) Floating lipid bilayers deposited on chemically grafted phosphatidylcholine surfaces, *Langmuir, 24, (5),* 1989-1999.

30. Hughes, A.V., RasCal. 2013, *Sourceforge*.

31. Arteta, M.Y., Ainalem, M.L., Porcar, L., Martel, A., Coker, H., Lundberg, D., Chang, D.P., Soltwedel, O., Barker, R., and Nylander, T. (2014) Interactions of PAMAM Dendrimers with Negatively Charged Model Biomembranes, *J. Phys. Chem. B, 118, (45),* 12892-12906.

32. Tatur, S., Maccarini, M., Barker, R., Nelson, A., and Fragneto, G. (2013) Effect of Functionalized Gold Nanoparticles on Floating Lipid Bilayers, *Langmuir, 29, (22),* 6606-6614.

33. Clifton, L.A., Green, R.J., Hughes, A.V., and Frazier, R.A. (2008) Interfacial Structure of Wild-Type and Mutant Forms of Puroindoline-b Bound to DPPG Monolayers, *J. Phys. Chem. B, 112, (49),* 15907-15913.

34.   Pencer, J., Mills, T., Anghel, V., Krueger, S., Epand, R.M., and Katsaras, J. (2005) Detection of submicron-sized raft-like domains in membranes by small-angle neutron scattering, *Eur. Phys. J. E: Soft Matter Biol. Phys., 18, (4),* 447-458.

35.   Efron, B. and Tibshirani, R.J., *An introduction to the bootstrap.* 1993, New York ; London: Chapman & Hall.

36.   Hancock, R.E. and Rozek, A. (2002) Role of Membranes in the Actitivites of Cationic Peptides, *FEMS Microbiol. Lett., 206,* 143-149.

37.   Trevors, J.T. (2003) Fluorescent probes for bacterial cytoplasmic membrane research, *J. Biochem. Biophys. Methods, 57, (2),* 87-103.

38.   Johnston, M.D., Hanlon, G.W., Denyer, S.P., and Lambert, R.J.W. (2003) Membrane damage to bacteria caused by single and combined biocides, *J. Appl. Microbiol., 94,* 1015-1023.

39.   Pozo Navas, B., Lohner, K., Deutsch, G., Sevcsik, E., Riske, K.A., Dimova, R., Garidel, P., and Pabst, G. (2005) Composition dependence of vesicle morphology and mixing properties in a bacterial model membrane system, *Biochim. Biophys. Acta, 1716, (1),* 40-48.

40.   Ranck, J.L. and Tocanne, J.F. (1982) Polymyxin-B Induces Interdigitation in Dipalmitoylphosphatidylglycerol Lamellar Phase with Stiff Hydrocarbon Chains, *FEBS Lett., 143, (2),* 175-178.

41.   Helfrich, W. (1978) Steric Interaction of Fluid Membranes in Multilayer Systems., *Z. Naturforsch., 33A,* 305-315.

42.   Fernandez, D.I., Le Brun, A.P., Whitwell, T.C., Sani, M.A., James, M., and Separovic, F. (2012) The antimicrobial peptide aurein 1.2 disrupts model membranes via the carpet mechanism, *Phys. Chem. Chem. Phys., 14, (45),* 15739-15751.

43.   Hobbs, J.K., Miller, K., O'Neill, A.J., and Chopra, I. (2008) Consequences of daptomycin-mediated membrane damage in *Staphylococcus aureus*, *J. Antimicrob. Chemother., 62, (5),* 1003-1008.

44.   Ooi, N., Miller, K., Hobbs, J., Rhys-Williams, W., Love, W., and Chopra, I. (2009) XF-73, a novel antistaphylococcal membrane-active agent with rapid bactericidal activity, *J. Antimicrob. Chemother., 64, (4),* 735-740.

45.   Danner, S., Pabst, G., Lohner, K., and Hickel, A. (2008) Structure and thermotropic behavior of the *Staphylococcus aureus* lipid lysyl-dipalmitoylphosphatidylglycerol, *Biophys. J., 94, (6),* 2150-2159.

46.   Sievers, S., Ernst, C.M., Geiger, T., Hecker, M., Wolz, C., Becher, D., and Peschel, A. (2010) Changing the phospholipid composition of *Staphylococcus aureus* causes distinct changes in membrane proteome and membrane-sensory regulators, *Proteomics, 10, (8),* 1685-1693.

47.   Castillo, J.A., Pinazo, A., Carilla, J., Infante, M.R., Alsina, M.A., Haro, I., and Clape, P. (2004) Interaction of Antimicrobial Arginine-Based Cationic Surfactants with Liposomes and Lipid Monolayers, *Langmuir, 20,* 3379-3387.

48.   Oku, Y., Kurokawa, K., Ichihashi, N., and Sekimizu, K. (2004) Characterization of the *Staphylococcus aureus* mprF gene, involved in lysinylation of phosphatidylglycerol, *Microbiol., 150, (Pt 1),* 45-51.

49.   Staubitz, P., Neumann, H., Schneider, T., Wiedemann, I., and Peschel, A. (2004) MprF-mediated biosynthesis of lysylphosphatidylglycerol, an important determinant in staphylococcal defensin resistance, *FEMS Microbiol. Lett., 231, (1),* 67-71.

50. Komljenovic, I., Marquardt, D., Harroun, T.A., and Sternin, E. (2010) Location of chlorhexidine in DMPC model membranes: a neutron diffraction study, *Chem. Phys. Lipids, 163, (6),* 480-487.

51. Zhang, T., Muraih, J.K., Tishbi, N., Herskowitz, J., Victor, R.L., Silverman, J., Uwumarenogie, S., Taylor, S.D., Palmer, M., and Mintzer, E. (2014) Cardiolipin prevents membrane translocation and permeabilization by daptomycin, *J. Biol. Chem., 289, (17),* 11584-11591.

52. Johnson, S.J., Bayerl, T.M., Wo, W.H., Noack, H., Penfold, J., Thomas, R.K., Kanellas, D., Rennie, A.R., and Sackmann, E. (1991) Coupling of Spectrin and Polylysine to Phospholipid Monolayers Studied by Specular Reflection of Neutrons, *Biophys. J., 60, (5),* 1017-1025.

53. Koenig, B.W., Kruger, S., Orts, W.J., Majkrzak, C.F., Berk, N.F., Silverton, J.V., and Gawrisch, K. (1996) Neutron reflectivity and atomic force microscopy studies of a lipid bilayer in water adsorbed to the surface of a silicon single crystal, *Langmuir, 12, (5),* 1343-1350.

54. Sackmann, E. (1996) Supported membranes: Scientific and practical applications, *Science, 271, (5245),* 43-48.

55. Wong, J.Y., Park, C.K., Seitz, M., and Israelachvili, J. (1999) Polymer-cushioned bilayers. II. An investigation of interaction forces and fusion using the surface forces apparatus, *Biophys. J., 77, (3),* 1458-1468.

56. Fragneto, G., Charitat, T., Graner, F., Mecke, K., Perino-Gallice, L., and Bellet-Amalric, E. (2001) A fluid floating bilayer, *Europhys. Lett., 53, (1),* 100-106.

57. Pabst, G., Danner, S., Karmakar, S., Deutsch, G., and Raghunathan, V.A. (2007) On the propensity of phosphatidylglycerols to form interdigitated phases, *Biophys. J., 93, (2),* 513-525.

58. Pan, J.J., Heberle, F.A., Tristram-Nagle, S., Szymanski, M., Koepfinger, M., Katsaras, J., and Kucerka, N. (2012) Molecular structures of fluid phase phosphatidylglycerol bilayers as determined by small angle neutron and X-ray scattering, *Biochim. Biophys. Acta, 1818, (9),* 2135-2148.

59. Nagle, J.F. and Tristram-Nagle, S. (2000) Structure of lipid bilayers, *Bioch. Biophys. Acta, 1469, (3),* 159-195.

Tables

Table 1 Kinetic parameters derived from the curve fitting functions applied to air/water interface monolayer surface pressure changes induced by interaction with HT61 following subphase injection.

Monolayer	$\Delta\Pi_{max}$ (mN/m)	t_{50} (s)	Hill coefficient	R^2
POPC	~0.4*	-	-	-
POPC/Chol	2.9	39.9	1.04	0.97
POPC/POPG (0 – 35 s)	5.4	15.5	1.40	0.99
POPC/POPG (17 – 300 s)	13.7	58.5	8.77	0.99

*Mean value obtained from the curve in Figure 1.

Table 2 Parameters of the characterisation of the three d_{62}DPPC/d_{62}DPPG bilayers obtained from the fitted reflectivity profiles and associated SLD profiles, prior to challenge with HT61 and after the first and second additions of HT61.

Data fitting parameters	d_{62}DPPC/d_{62}DPPG Bilayer Composition (mol%)								
	[75:25]			[50:50]			[25:75]		
	Alone	HT61 (1)	HT61 (2)	Alone	HT61 (1)	HT61 (2)	Alone	HT61 (1)	HT61 (2)
CW thickness (Å)	17.7 ± 3.3	11.7 ± 1.7	28.6 ± 3.2	83.5 ± 4.5	55.6 ± 5.3	27.5 ± 9.3	113.4 ± 8.2	62.6 ± 5.1	67.1 ± 5.2
Bilayer APM (Å²)	102.9 ± 3.6	112.3 ± 2.2	118.6± 3.9	90.6 ± 4.0	106.9 ± 3.8	103.1 ± 7.1	97.4 ± 4.4	119.9 ± 3.2	340 ± 100
H₂O/head	34.8 ± 5.8	21.4 ± 0.6	20.7 ± 3.9	13.3 ± 1.7	23.9 ± 9.8	34.4 ± 8.4	4.9 ± 3.1	39.6 ± 5.2	39.3 ± 9.1
H₂O/tail	0.6 ± 2.1	10.0 ± 0.8	20.9 ± 3.8	0.0 ± 4.0	16.9 ± 4.5	28.6 ± 3.9	0.0 ± 1.8	20.6 ± 4.4	70.7 ± 20.2
Global roughness (Å)	34.4 ± 1.8	34.7 ± 1.3	23.6 ± 1.1	22.5 ± 1.1	18.0 ± 2.5	27.5 ± 4.5	26.5 ± 1.1	26.4 ± 2.1	40.0 ± 9.7
Local roughness (Å)	4.4 ± 2.7	1.9 ± 1.1	2.5 ± 0.3	1.0 ± 4.5	0.2 ± 3.6	1.1 ± 4.8	0.3 ± 1.0	0.5 ± 2.1	4.1 ± 4.0
*Layer thickness (Å)	44.4 ± 3.0	38.4 ± 1.2	41.6 ± 3.4	35.6 ± 4.4	45.6 ± 4.4	60.2 ± 7.0	28.0 ± 2.6	50.4 ± 3.8	26.6 ± 8.1
*Tail % hydration	2.0 ± 6.5	25.2 ± 10.2	41.3 ± 32.4	0.0 ± 11.9	36.2 ± 26.3	49.0 ± 47.6	0.0 ± 5.7	49.9 ± 32.3	70.4 ± 100

*Parameters derived from the fitted models.

Figure legends

Figure 1: Increase in fluorescence of $DiSC_3(5)$ dye from a (A) logarithmic and (B) stationary phase culture of *S. aureus* with an OD_{600} of 0.05 after exposure to various concentrations (32, 16, 8, 4, 2, 1, 0.5 and 0 µg/ml) of HT61 (filled triangles), chlorhexidine (filled squares) and penicillin G (filled circles) (5 mM HEPES 5 mM Glucose (pH 7.2)) for 20 minutes. Error bars represent the standard error of the mean (n=3).

Figure 2: Initial rate of depolarisation over the first minute of both HT61 (filled triangles) and chlorhexidine (filled squares) plotted against drug concentration for (A) logarithmic and (B) stationary phase *S. aureus*. Error bars represent the standard error of the mean (n=3).

Figure 3: Percentage ATP release from (A) logarithmic and (B) stationary phase *S. aureus* (OD_{600} 0.2) after 20 minutes exposure to HT61 (filled triangles), chlorhexidine (filled squares) and penicillin G (filled circles). Error bars represent the standard error of the mean (n=3).

Figure 4 Changes in air/water interface lipid monolayer surface pressures (n = 3 ± s.d.) in response to subphase injection of HT61 (~9 ug/ml), for monolayers composed of POPC (black circles), POPC/Chol [75:25] (brown squares) and POPC/POPG [75:25] (dark green diamonds). The solid lines represent curves fitted to the data using a three-parameter Hill function (light green line) for the POPC/Chol monolayer or a piecewise fitting using both a three-parameter Hill function (0 – 35 s) and a four-parameter sigmoidal function (17 – 300 s) (red lines) for the POPC/POPG monolayer.

Figure 5 Neutron reflectivity curves showing only the modelled fits (A, B, C) and corresponding derived SLD profiles (D, E, F) of the SAM and floating bilayer in H_2O contrast alone for (A, D) the $d_{62}DPPC:d_{62}DPPG$ [75:25] bilayer ($\chi^2 = 119.0$), (B, E) the

d_{62}DPPC:d_{62}DPPG [50:50] bilayer ($\chi^2 = 156.6$), and (C, F) the d_{62}DPPC:d_{62}DPPG [25:75] bilayer ($\chi^2 = 124.8$). For each bilayer composition, the reflectivity from the unchallenged bilayers is compared with that obtained after the first and second additions of HT61.
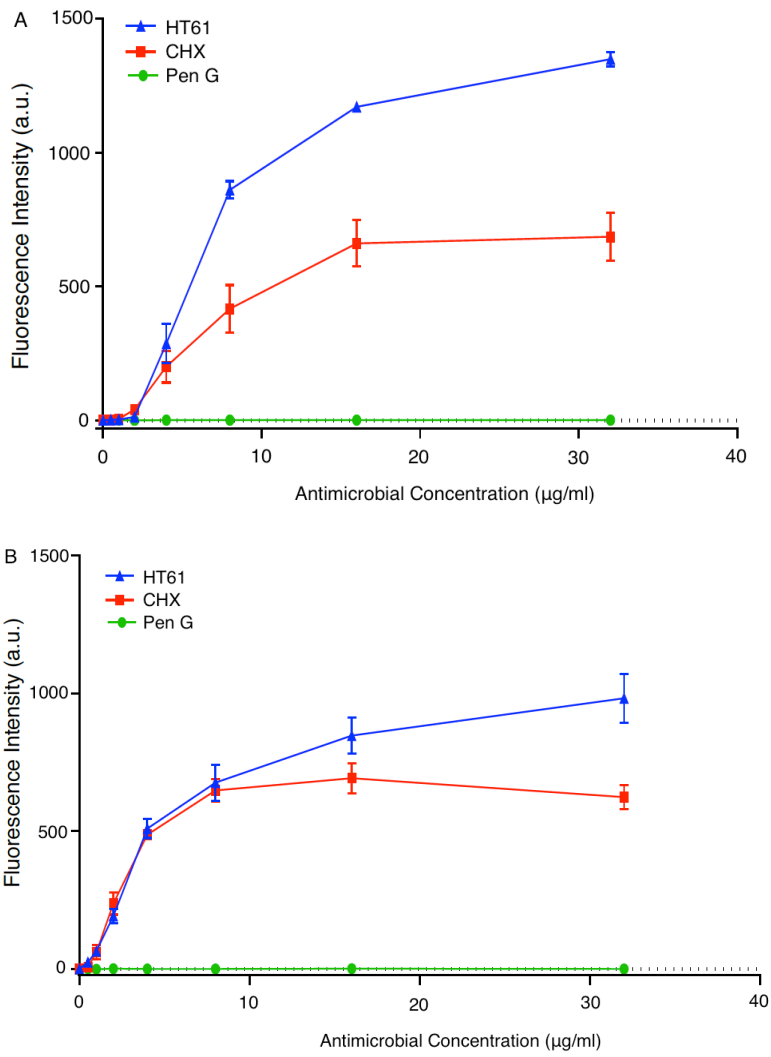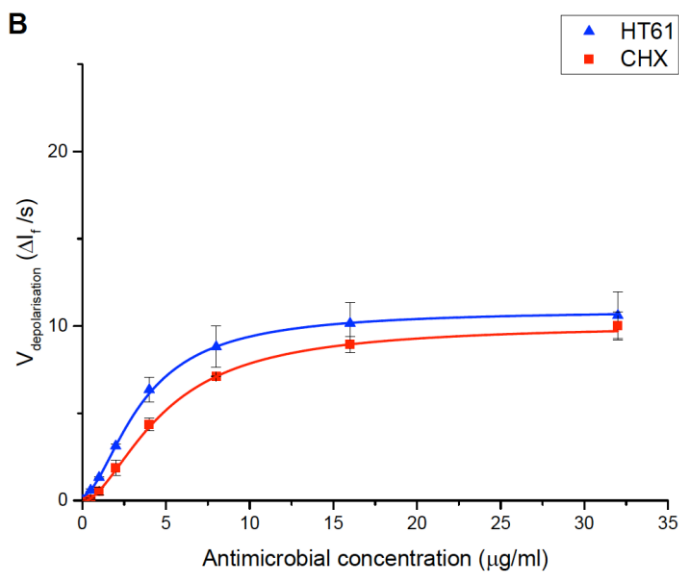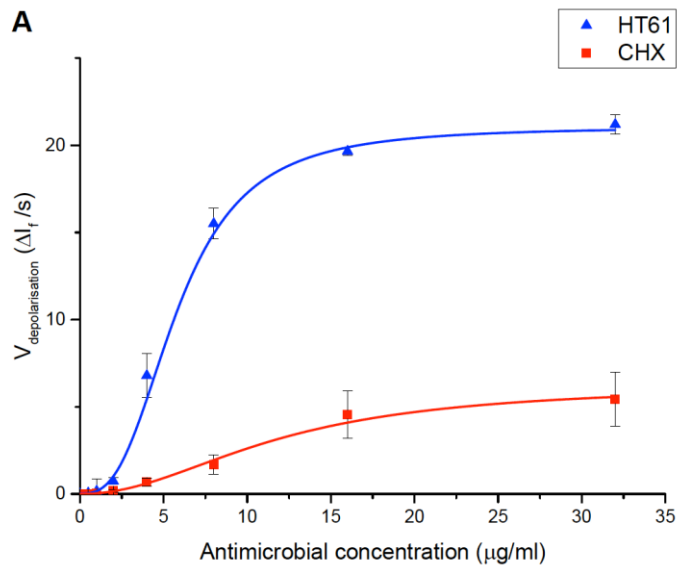
Figures

Figure 1
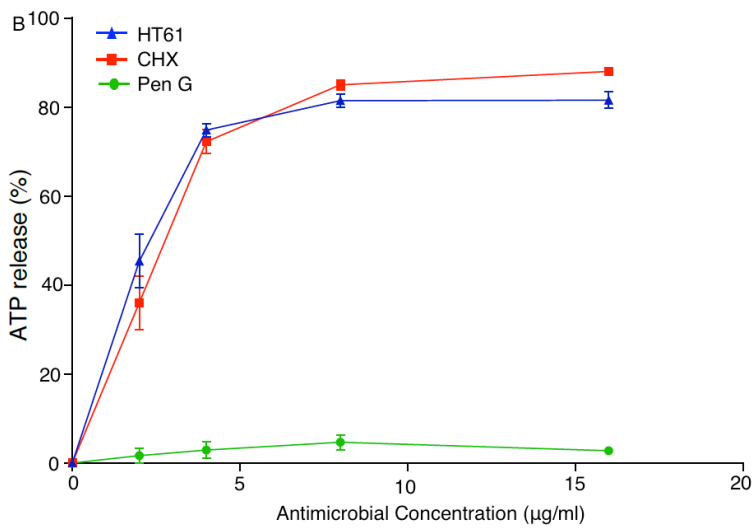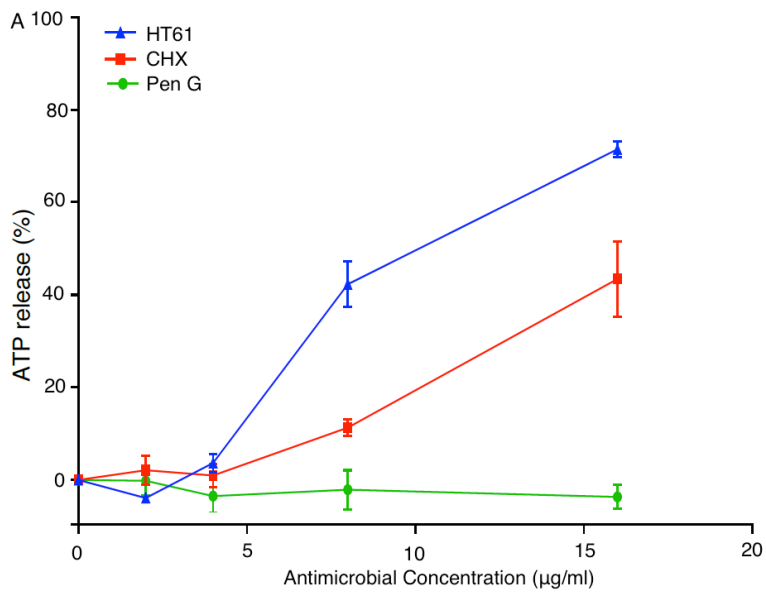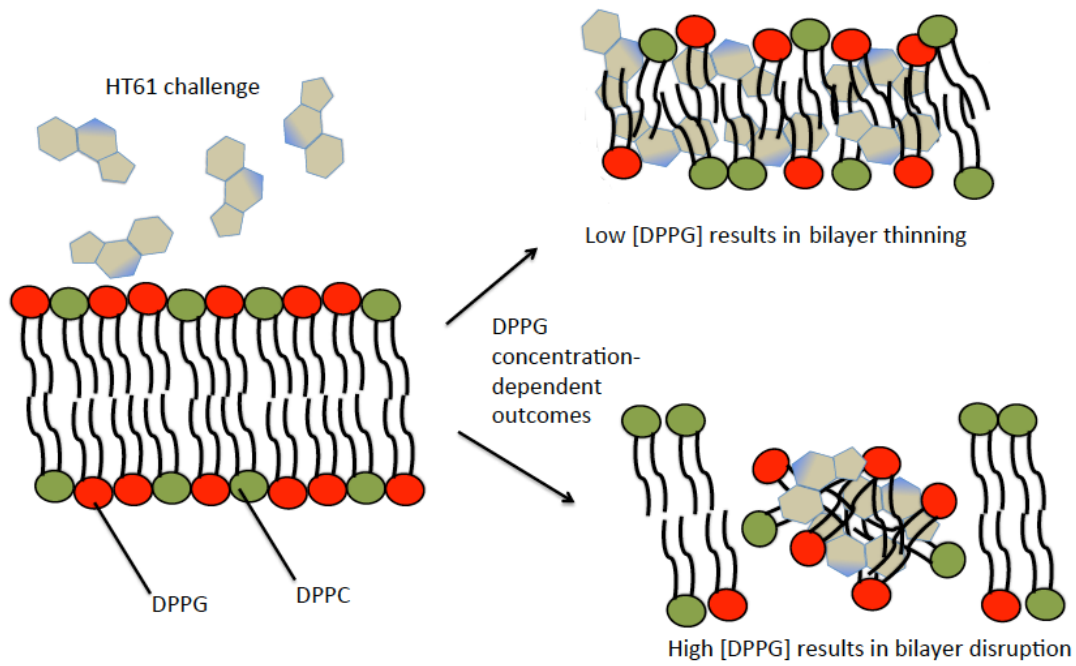
Figure 2

Figure 3
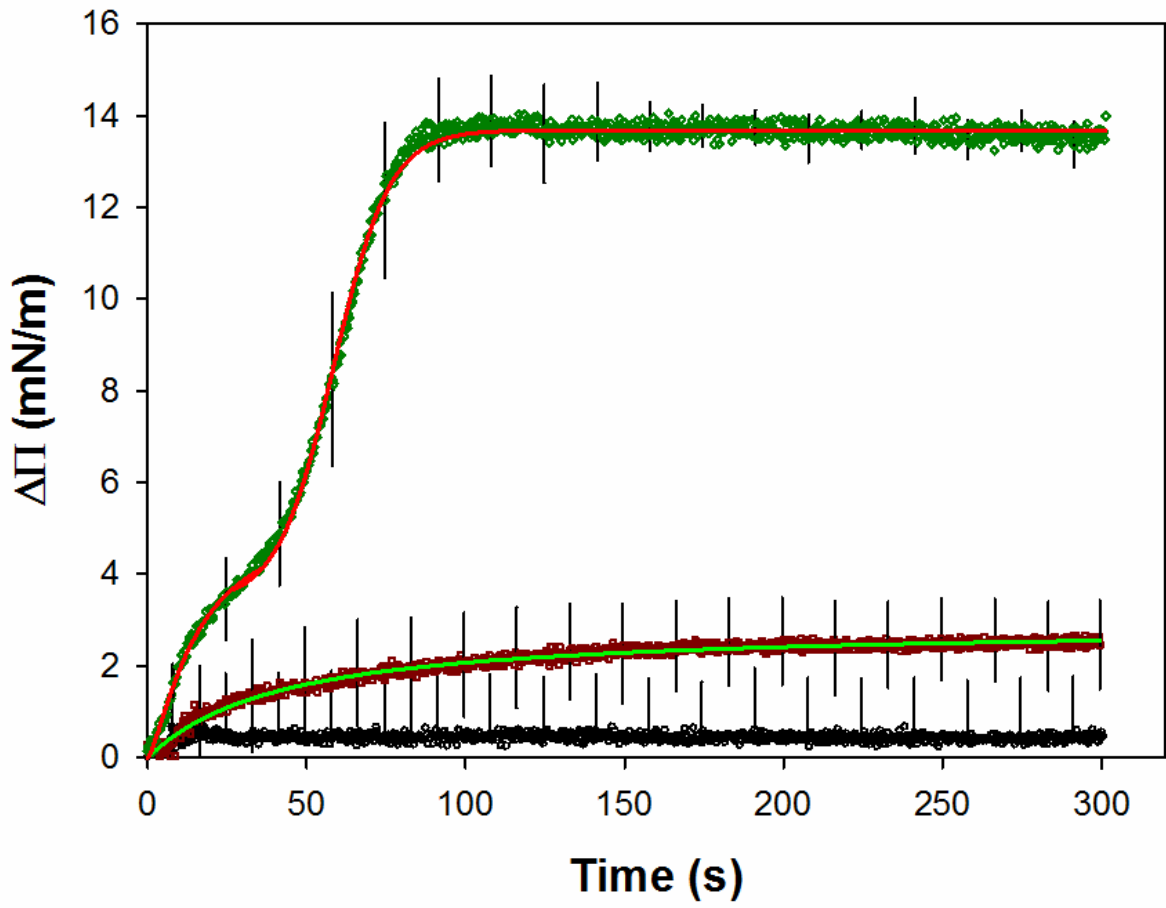
Figure 4
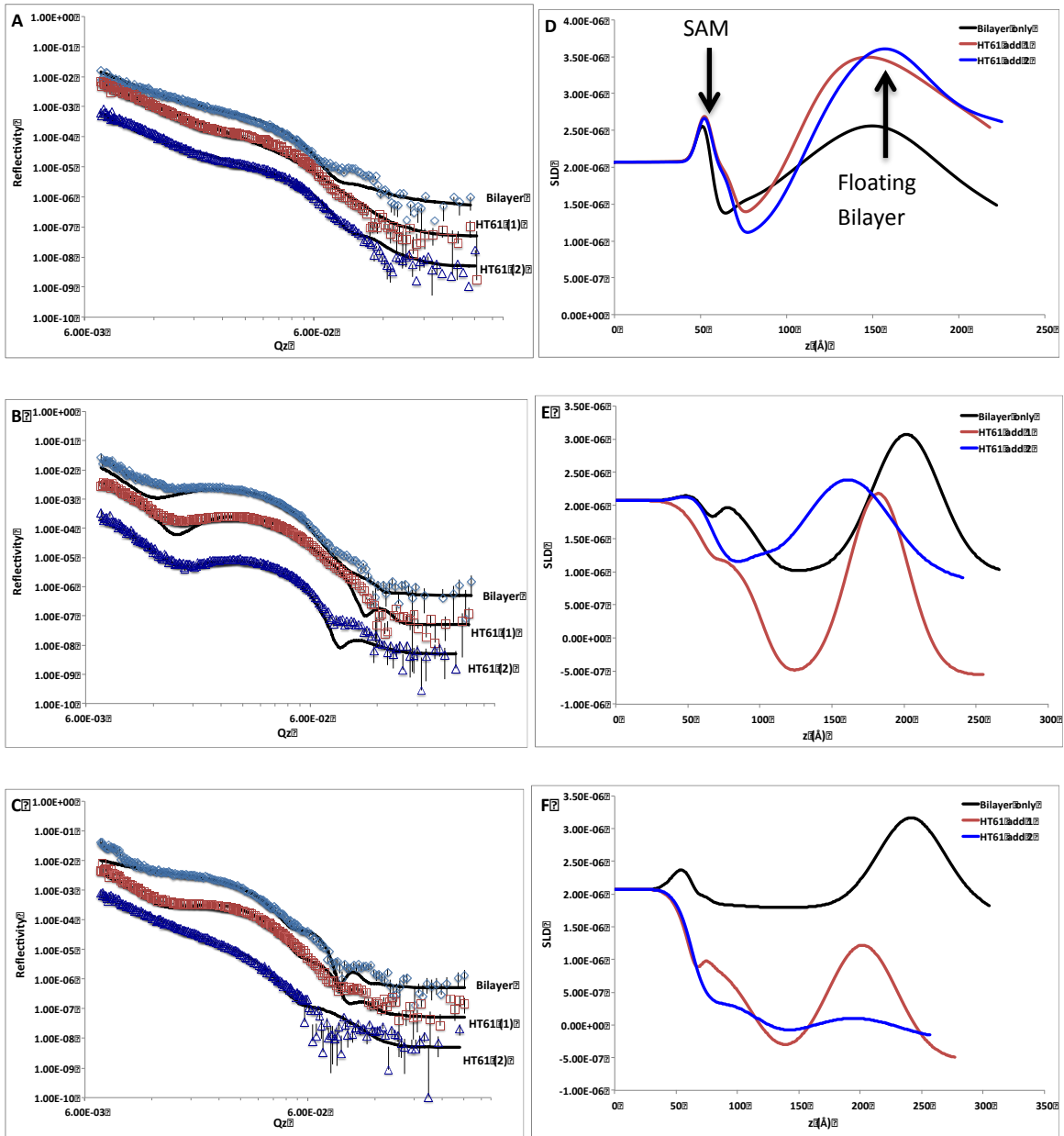
Figure 5

For Table of Contents Use Only

The mechanism of action of a membrane-active quinoline-based antimicrobial on natural and model bacterial membranes

Alasdair T. M. Hubbard · Robert Barker · Reg Rehal · Kalliopi-Kelli A. Vandera · Richard D. Harvey · Anthony R. M. Coates

Supporting Information

The mechanism of action of a membrane-active quinoline-based antimicrobial on natural and model bacterial membranes

Alasdair T. M. Hubbard[1, a] · Robert Barker[3, b] · Reg Rehal[2] · Kalliopi-Kelli A. Vandera[2] · Richard D. Harvey[2, c] · Anthony R. M. Coates[1]*

[1]*Medical Microbiology, Institute for Infection and Immunity, St George's, University of London, Cranmer Terrace, London SW17 ORE, UK.*

[2]*Institute of Pharmaceutical Science, King's College London, Franklin Wilkins Building, 150 Stamford Street, London SE1 9NH, UK.*

[3]*Institut Laue Langevin, 71 avenue des Martyrs, 38042 Grenoble, France.*

*Corresponding author: e-mail acoates@sgul.ac.uk

Current affiliations:

[a]*Nuffield Department of Clinical Medicine, University of Oxford, Oxford, United Kingdom OX3 9DU*

[b]*School of Science and Engineering, University of Dundee, Dundee DD1 4HN, UK.*

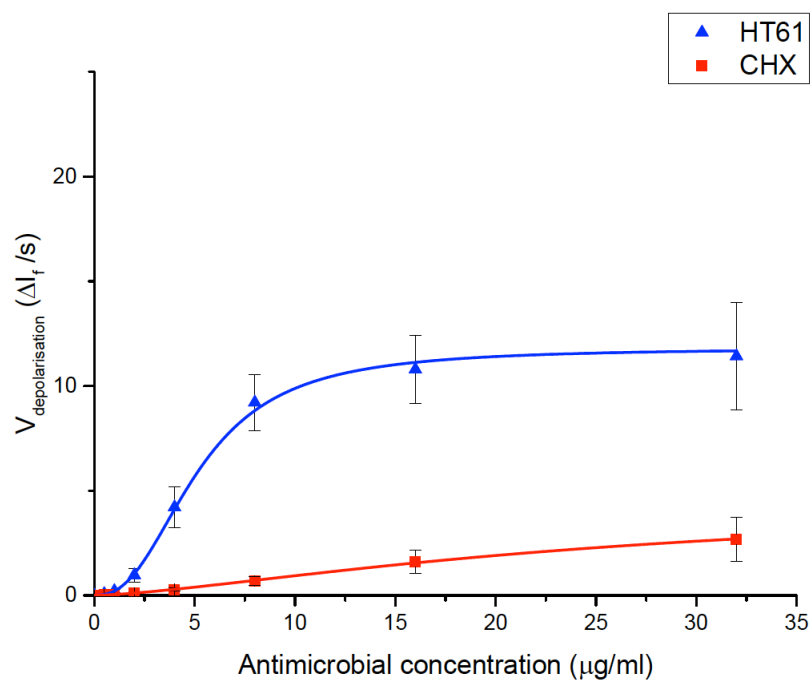[c]*Institute of Pharmacy, Martin Luther University Halle-Wittenberg, Halle (Saale), Germany.*

Figure S1 Initial rate of depolarisation over the first minute of both HT61 (filled triangles) and chlorhexidine (filled squares) plotted against drug concentration for logarithmic phase daptomycin resistant *S. aureus*. Error bars represent the standard error of the mean (n=3). The curves are fitted with the sigmoidal Hill function described in eqn 6. The kinetic parameters obtained from the curve fitting were in the case of HT61; $Vdep_{max}$ 11.8 s^{-1}, K_m 5.2 µg/ml and for chlorhexidine; $Vdep_{max}$ 4.7 s^{-1}, K_m 25.9 µg/ml.

Table S1 Parameters of the characterisation of the three SAM layers (indicating the specific floating bilayer with which they were associated) obtained from their fitted reflectivity profiles.

Associated d_{62}DPPC/d_{62}DPPG bilayer	Layer of model	Thickness (Å)	Roughness (Å)	Hydration (%)
75:25	Si substrate		4.0 ± 0.3	
	SiO$_2$	5.0 ± 0.3	4.0 ± 0.3	0 ± 3.5
	TMPA	14.0 ± 0.8	4.0 ± 0.4	55.0 ± 0.9
	al-PC Chains	31.9 ± 1.0	15.8 ± 1.0	24.7 ± 0.9
	al-PC Heads	9.0 ± 0.0[a]	15.8 ± 1.0[b]	10.2 ± 0.3
50:50	Si substrate		10.0 ± 1.7	
	SiO$_2$	16.0 ± 1.4	10.0 ± 1.7	43.8 ± 2.2
	TMPA	5.4 ± 3.3	5.0 ± 2.4	24.6 ± 6.9
	al-PC Chains	23.4 ± 1.1	10.5 ± 2.7	31.7 ± 7.5
	al-PC Heads	9.0 ± 0.0[a]	10.5 ± 2.7[b]	36.1 ± 4.2
25:75	Si substrate		8.4 ± 1.4	
	SiO$_2$	14.7 ± 0.5	8.4 ± 1.4	45.0 ± 2.5
	TMPA	5.1 ± 2.8	4.0 ± 3.0	60.0 ± 8.2
	al-PC Chains	35.0 ± 3.4	19.0 ± 2.1	30.3 ± 2.1
	al-PC Heads	9.0 ± 0.0[a]	19.0 ± 2.1[b]	37.4 ± 4.2

[a]Fixed value according to Hughes *et al*. (Hughes *et al.* 2008)

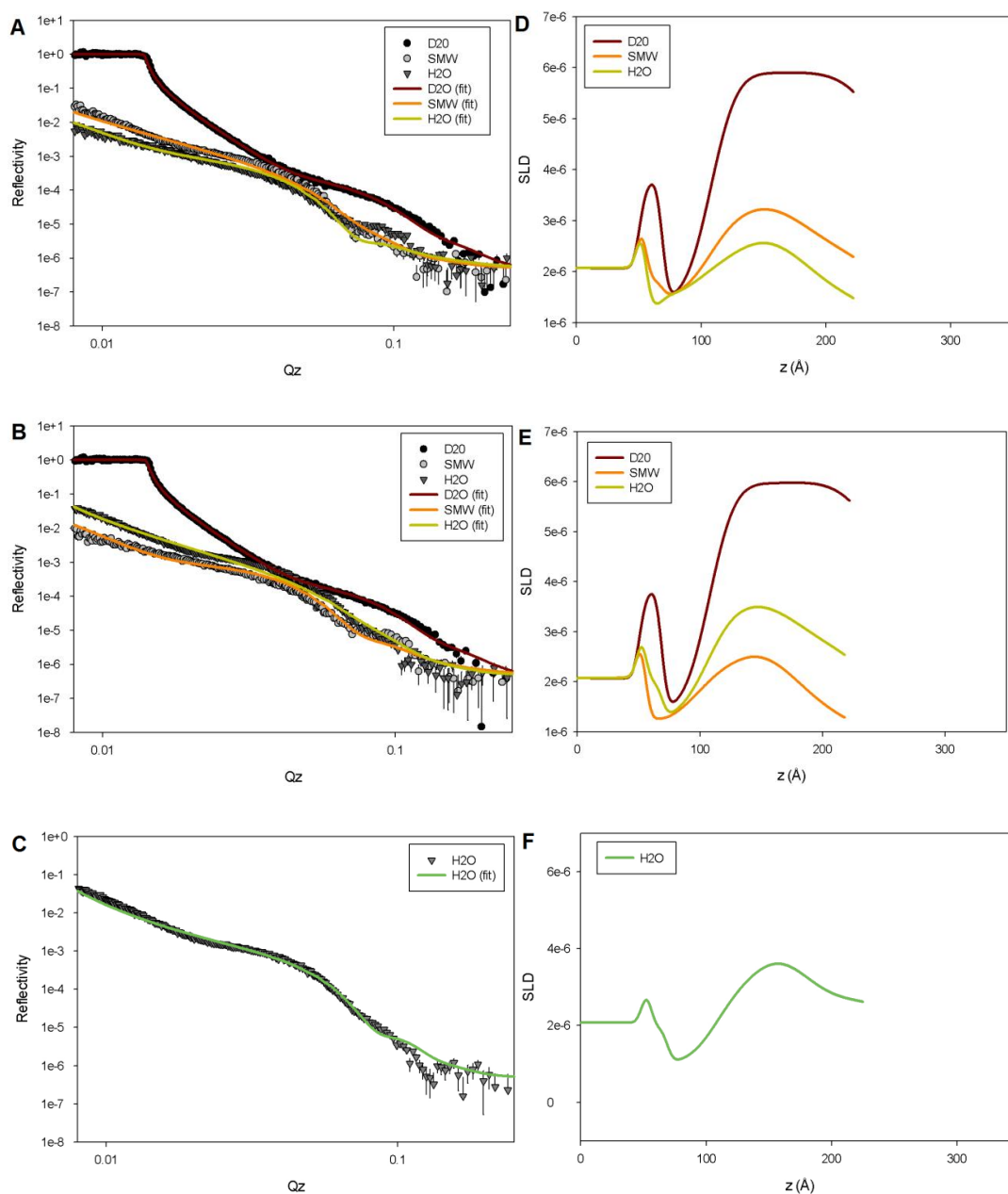[b]Fixed at the same value as the chain roughness.

Figure S2 Fitted neutron reflectivity curves (A, B, C) and derived SLD profiles (D, E, F) for the SAM and floating d_{62}DPPC/d_{62}DPPG [75:25] bilayer (A & D) pre-addition of HT61, (B & E) after the first addition of HT61 and (C & F) after the second addition of HT61. The Chi squared value for all three fits was 119.
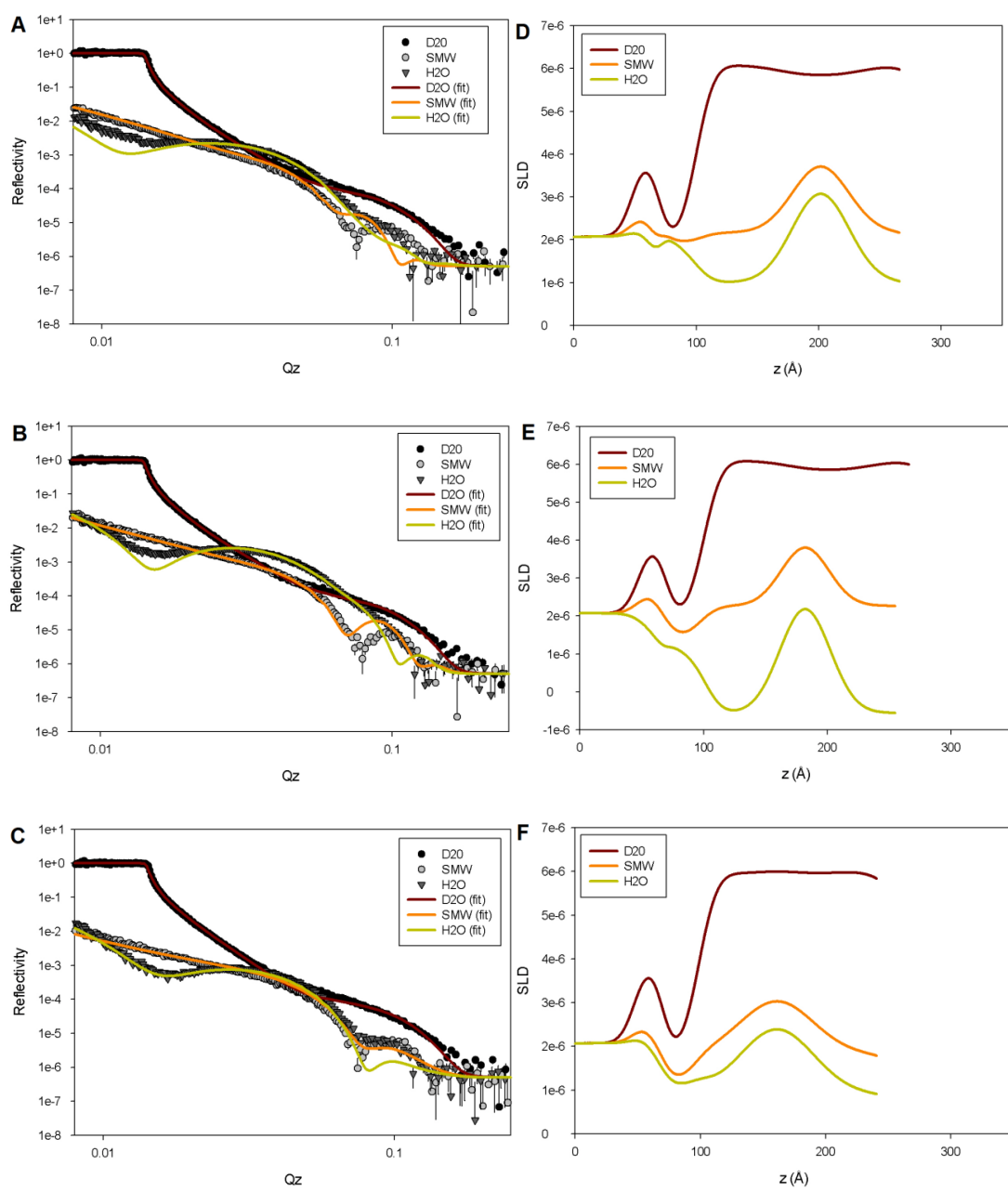
S4

Figure S3 Fitted neutron reflectivity curves (A, B, C) and derived SLD profiles (D, E, F) for the SAM and floating d_{62}DPPC:d_{62}DPPG [50:50] bilayer (A & D) pre-addition of HT61, (B & E) after the first addition of HT61 and (C & F) after the second addition of HT61. The Chi squared value for all three fits was 156.6.
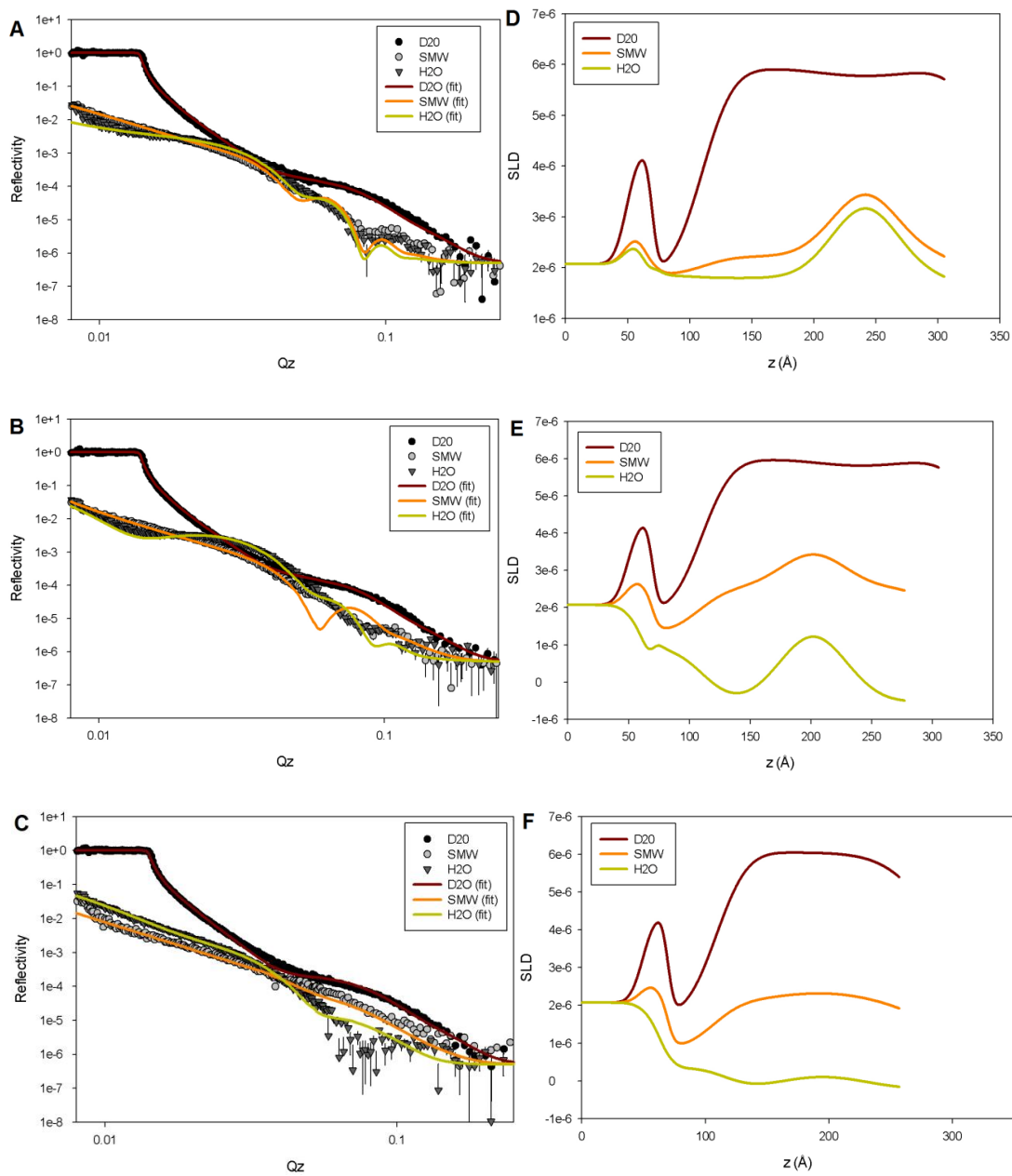
Figure S4 Fitted neutron reflectivity curves (A, B, C) and derived SLD profiles (D, E, F) for the SAM and floating d_{62}DPPC:d_{62}DPPG [25:75] bilayer (A & D) pre-addition of HT61, (B & E) after the first addition of HT61 and (C & F) after the second addition of HT61. The Chi squared value for all three fits was 124.8.